Title	Heat conduction analyses on rewetting front propagation during transients beyond anticipated operational occurrences for BWRs
Author(s)	Yonomoto Taisuke, Shibamoto Yasuteru, Satou Akira, Okagaki Yuria
Citation	Journal of Nuclear Science and Technology, 53(9), p.1342-1352
Text Version	Author's Post-print
URL	https://jopss.jaea.go.jp/search/servlet/search?5053485
DOI	https://doi.org/10.1080/00223131.2015.1108882
Right	This is an Accepted Manuscript of an article published by Taylor & Francis in Journal of Nuclear Science and Technology on September 2016, available online: http://www.tandfonline.com/10.1080/00223131.2015.1108882.

ARTICLE

Heat conduction analyses on rewetting front propagation during transients beyond anticipated operational occurrences for BWRs

Taisuke Yonomoto*, Yasuteru Sibamoto, Akira Satou and Yuria Okagaki

Thermohydraulic Safety Research Group, Japan Atomic Energy Agency,

2-4 Shirakata, Tokai, Ibaraki, 319-1195, Japan

Acknowledgements

The experiment in this work was conducted under the auspices of the former Nuclear and Industrial Safety Agency in the Ministry of Economy, Trade and Industry of Japan.

Our previous study investigated the rewetting behavior of dryout fuel surface during transients beyond anticipated operational occurrences (AOOs) for BWRs, which indicated the rewetting velocity was significantly affected by the precursory cooling defined as cooling immediately before rewetting. The present study further investigated the previous experiments by conducting additional experimental and numerical heat conduction analyses to characterize the precursory cooling. For the characterization, the precursory cooling was firstly defined quantitatively based on evaluated heat transfer rates; the rewetting velocity was investigated as a function of the cladding temperature immediately before the onset of the precursory cooling. The results indicated that the propagation velocity appeared to be limited by the maximum heat transfer rate near the rewetting front. This limitation was consistent with results of the heat conduction analysis using heat transfer models for the precursory cooling expressed as a function of distance from the rewetting front, the maximum wetting temperature, and the heat transfer coefficients in the wetted region. This paper also discusses

uncertainties in the evaluation of transient heat flux from the measured surface temperature, and technical issues requiring further investigation.

Keywords; rewetting velocity; post-boiling transition; precursory cooling; heat conduction analysis; rod bundle; rewetting

*Corresponding author. Email: yonomoto.taisuke@jaea.go.jp

1. Introduction

The nuclear regulation authority of Japan recently initiated the development of a thermal-hydraulic system analysis code with objectives including facilitation of regulatory utilization of the latest technological findings obtained from the safety study. The thermohydraulic safety research group of the Japan Atomic Energy Agency (JAEA) supports the development by providing experimental databases for the code validation and technical knowledge obtained in the safety study. For this support, JAEA will conduct some new experiments for the technical issues which have significant safety importance but insufficient technical knowledge for the regulatory use. As an approach to find such technical issues, we are investigating the previous studies including those conducted by JAEA or the former Japan atomic energy research institute.

This paper describes one of such efforts on the reinvestigation, which focuses on the post-boiling transition (Post-BT) heat transfer experiments conducted from 2005 to 2009. The Post-BT behavior was one of significant technical and regulatory issues after the publication of the Post-BT standard by the Atomic Energy Society of Japan (AESJ) in 2003 [1]. This standard proposed the allowance of the core dryout under conditions limited by the duration and maximum cladding temperature during AOOs for the BWR licensing. The standard also proposed evaluation methods for the Post-BT thermal-hydraulic behavior: dryout initiation, Post-BT heat transfer, and rewetting front propagation.

Motivated by the importance of the AESJ standard on the licensing and insufficient studies on high-pressure and high-heat flux rewetting, our research group initiated the research on the Post-BT, focusing on the rewetting front propagation and heat transfer. Two test facilities were developed for this study: single-tube heat transfer test facility and 2x2 bundle test facility. By using both facilities, steady-state and transient experiments were conducted under simulated BWR thermal hydraulic conditions to obtain Post-BT heat transfer rates, deposition rates of liquid droplets for the annular-mist flow regime, and the rewetting

behavior after the core dryout [2-4]. Rewetting behavior was also studied by analytically solving the two-dimensional transient heat conduction equation. The obtained analytical equations clarified a relation among the rewetting velocity, the hot wall temperature, and the heat transfer rates in the precursory cooling and wetted regions. Here, the precursory cooling is defined as cooling in the dryout region just before the rewetting.

From those experimental and analytical studies, several conclusions were obtained for the rewetting front propagation including: 1) When the precursory cooling was not modeled, the rewetting velocity was underpredicted significantly, and 2) When the precursory cooling was appropriately modeled as a function of the distance from the rewetting front and using a set of heat transfer correlations, the experimental data were predicted well by the model, although the required set of heat transfer correlations were not investigated in detail.

Since the post-BT behavior is important also for the accident analysis including anticipated transient without scram which should be discussed in the safety review for the regulation revised after the Fukushima Dai-ichi nuclear power plant accident, we have reinvestigated the experimental results to identify remained technical issues and clarify the necessity of the additional experimental study. For this purpose, multidimensional heat conduction analysis was newly conducted to obtain the heat flux from the measured surface temperature and clarify parameter effects on the rewetting front propagation. Results of those investigations are described in this paper.

2. Summary of Previous Experiments

2.1. Post-BT Bundle Test Facility

The facility consisted of a test section, a water circulation loop, a steam condenser, and systems for power supply, instrumentation and control. The test section was designed to simulate the 9x9 BWR fuel bundle and consists of 2x2 simulated heater rods with diameter of 11.2mm, heated length of 3.71 m, and chopped cosine power profile. The heater rods were

arrayed with a pitch of 14.3 mm and fastened together with simulated cell-type spacers at seven vertical locations. Those spacers are provided by nuclear fuel manufacturers which fabricate the actual BWR 9x9 bundle. **Figures** 1 and 2 show the crosssectional view of the test bundle and heater rods, respectively.

The measurements included pressure, fluid temperature, flow rate, power, and heater rod surface temperature. The heater rod surface temperatures were measured with sheathe-type thermo-couples(T/Cs) embedded in the rod cladding at an interval of 30 degree angle in the peripheral direction and wired either from the bottom or top. The cladding material of the sheathe-type T/C was INCONEL with thickness of 50μm and diameter of 500μm. Inside the sheath cladding, chromel and alumel wires with diameter of 50μm were installed with the powdered MgO as electrical insulator. The temperature sense region, i.e., the contact point of the two metals, had the size of approximately 50μm and located in the radial center and 250μm from the front end of the sheath.

Each heater rod had 24 T/Cs with different peripheral and vertical measurement locations. Since the dryout tends to occur in the upper part of the core, the surface temperatures were densely measured at the minimum vertical interval of 20mm among 5th, 6th and 7th spacers which were installed at 1208, 696 and 184 mm from the core top, respectively. The T/Cs on the rod A and B were installed between 6th and 7th, and 5th and 6th spacers, respectively; those on the rod C and D were installed between 5th and 7th spacers. The data was recorded at the sampling speed of 100 Hz.

2.2. Test Procedure and Conditions

Four types of tests were conducted: 1) steady state tests for measurements of critical heat fluxes, Post-BT heat transfer coefficients and deposition rates of liquid droplets, 2) dryout transient tests initiated either by an increase of the power or a decrease of the flow rate from a steady-state condition, 3) rewetting transient tests initiated either by a decrease of the

power or an increase of the flow rate, and 4) AOO simulation tests. Rewetting transient tests conducted at 7 MPa are described in this paper, of which test conditions are summarized in **Table** 1. The test conditions are based on the AOO conditions in a BWR.

The rewetting front velocity was evaluated from the rewetting timings and a data fitting assuming a quadratic relation between the rewetting timing and the thermocouple elevation. The rewetting timing was determined as a time when the evaluated heat flux took a maximum. The heat flux was evaluated from the measured surface temperature using a simplified analysis model to solve the inverse problem. Details of the data processing are available in the reference [2].

2.3. Rewetting Transient Test Results

2.*3.1. Initial steady-state behavior*

When the core power was increased or the flow rate was decreased step-wisely, the dryout always initiated from the immediate upstream of the 7th spacer located at 184mm from the core top. **Figure** 3 shows the typical vertical temperature distributions observed at the rod C and D (see Figure 1 for the rod identifier). Three curves in Figure 3 correspond to the temperatures observed at the surface facing the center, side and corner flow channel (see Figure 1 for the definition of each flow channel). Figure 3 shows a tendency that the temperatures are lower in the downstream of the spacer and higher in the upstream, indicating the heat transfer enhancement at the spacer. It also shows the surface temperatures have a peripheral distribution probably affected by the non-heated channel box wall. The temperatures are typically higher for the surfaces facing the channel box. The peripheral temperature distributions with the difference of more than 100 K were occasionally observed on the same rod.

2.3.2. General behavior of rewetting front propagation

Figure 4 shows typical rewetting front propagation behaviors measured between 6th

and 7th spacers at the rod A for four experiments, where each symbol corresponds to the rewetting timing at the measured elevation for each experiment. Relatively large variation of the propagation velocity is shown in the lower part of the measured region (between 0.4 and 0.7 m in Figure 4). On the other hand, the rewetting front propagated at almost the constant velocity in the upper part (between 0.2 and 0.4 m in Figure 4). For the rod A, the temperatures were measured for the surfaces facing only the center channel in the upper part, while the data measured for the surfaces facing the different flow channels were included in the lower part. Since the rewetting behavior observed for the rod C and D typically shows a propagation at a constant velocity for the surface facing the same flow channel in the entire region between the two spacers, the different rewetting behavior in the upper and lower regions observed for the rod A was probably caused by the measurement location difference in the peripheral direction. That is, the rewetting velocity in the upper part of the region between 6th and 7th spacers was constant for the rod A probably because the temperature measurement locations faced only the center channel in the upper part.

Similar behavior was observed for the rod B, for which the almost constant propagation was observed in the upper part of the region between 5th and 6th spacers due to the same reason for the rod A. Rewetting behavior observed in the upper part between adjacent spacers for the rod A and B will be presented hereafter in order to characterize the basic nature of the rewetting front propagation.

3. Heat Conduction Analysis

3.1. Analysis Procedures

Three types of heat conduction analyses were conducted for 1) the clarification of parameter effects on the rewetting front propagation, 2) the evaluation of heat transfer coefficient from the measured cladding surface temperature, and 3) the evaluation of the uncertainty of the duration of the precursory cooling.

3.1.1. Parametric study on rewetting front propagation

Two-dimensional heat conduction behavior in the rod was analyzed assuming steady state in the cylindrical coordinate system fixed on the rewetting front and uniformity in the peripheral direction. For those assumptions, the heat conduction equation can be expressed as:

$$\rho c u_R \frac{\partial T}{\partial z} + \nabla\left(k \nabla T\right) + S = 0 \qquad (1)$$

where ρ is density, c specific heat, u_R the rewetting velocity, T temperature, k thermal conductivity, and S volumetric power density. A discretization scheme for the equation was based on the control-volume formulation used in thermal-hydraulic analysis codes such as COBRA [5]. Inner structures of the heater rod: the boron nitride insulator, Nichrome heater element, and Inconel cladding were taken into account in the analysis. The property of the structure was given as a function of the temperature. A system of the discretization equations were solved iteratively using an open-source mathematical library of "The Matrix Toolkits for Java (MTJ)" [6].

The boundary condition on the heater rod surface was calculated using the heat transfer correlations: the Chen correlation [7] for the wetted region, the Groeneveld 5.9 correlation [8] for the dryout region for the base case, and a linear interpolation for the precursory cooling region expressed as

$$q_{PC} = -\left(q_{rewet} - q_{dry}\right)\frac{z}{L} + q_{rewet} \qquad \text{for } 0<z<L \qquad (2)$$

where z is the distance from the rewetting front, L the length of the precursory cooling, q_{rewet} heat flux at the rewetting front, and q_{dry} the heat flux for the dryout region. The maximum superheat temperature was evaluated by the Lienhard model [9] for the base case, which gives a value of 46 K at pressure of 7MPa. It should be noted that the applicability of those correlations to the present condition is not clear as will be discussed in Section 5.3. The present analysis, however, is found to be useful to understand characteristics of the observed

rewetting behavior and identify unresolved technical issues.

From a given set of initial and boundary conditions, any temperature can be calculated at the rewetting front, if not controlled. In order to avoid unrealistically high temperature at the rewetting front, the calculated rewetting velocity was iteratively adjusted to have the predetermined rewetting temperature using the Newton method. The rewetting velocity calculated using this method can be regarded as the maximum velocity controlled by the limitation of the maximum liquid temperature.

Fluid conditions of pressure, temperature, mass flux and quality were assumed to be constant in the flow direction to simplify the boundary condition. The base case calculation conditions are summarized in **Table** 2.

3.1.2. Evaluation of heat transfer coefficient from the temperature data

The heat flux at the rod surface was evaluated from the analysis of the one-dimensional (1-D) heat conduction in the radial direction. Since the T/C measuring location was 250 μm below the surface of the heater rod with a radius of 5.6mm, a virtual cylindrical region with a radius of 5.35mm was calculated using the measured data as a boundary condition. The surface heat flux and cladding temperature were extrapolated from the calculated values at the virtual heater rod surface. The used assumption of the one-dimensional in the radial direction can be justified because the axial heat conduction is of little importance for the present tested conditions characterized by high-pressure and high-heat flux [4].

3.1.3. Uncertainty of evaluated precursory cooling duration

The duration of the precursory cooling was evaluated based on the change of the heat transfer coefficient and the peak heat flux as will be described in the next section. The surface temperature measurement is generally affected by errors caused by 1) the measurement location different from the surface, 2) the size of the temperature sense region, 3) the different physical properties inside the thermocouple sheath, and so on. The uncertainty caused by

those errors was analyzed based on the three-dimensional (3-D) heat conduction analysis using the Euler coordinate system fixed on the heater rod, because of the axial asymmetry of the T/C sheath geometry at the measurement elevation.

Procedure for the uncertainty evaluation was as follows: 1) the 3-D analysis was conducted, where the time-dependent movement of the rewetting front was considered by giving the heat transfer coefficient as functions of time, temperature and the distance from the wetting front, 2) from the result of the 3-D analysis, a simulated T/C data was produced by averaging the temperatures in the temperature sense region, 3) the simulated T/C data was used as a boundary condition for the 1-D analysis using the same procedure as the evaluation of the heat transfer coefficient from the measured data, 4) the calculated surface heat flux responses were compared between the 3-D and 1-D analyses focusing on the heat flux and surface temperature.

4. Experimental Data Analysis

4.1. Characterization of Precursory Cooling

Figure 5 shows all the temperature responses measured at 0.821m from the core top for the rod B for the rewetting tests conducted at 7 MPa, in which the time zero corresponds to the rewetting time. Figure 5 shows rapid temperature decreases immediately before the rewetting, which are caused by the precursory cooling. In order to characterize the precursory cooling, it is necessary to quantitatively define the onset of the precursory cooling. From the definition, the onset of the precursory cooling may be represented by a time when the heat transfer coefficient definitely exceeds that before the precursory cooling. This time may be determined using a value of the typical heat transfer coefficient before rewetting multiplied by an experimentally determined factor. After many trials, the typical heat transfer coefficient before the precursory cooling was obtained from the average between 1 and 2 second before rewetting.

Figures 6 and 7 show a typical response of the heat transfer coefficient and surface temperature, respectively, compared with the onset timings for the precursory cooling defined with multipliers of 1.3, 2, and 3. For this comparison, the timing determined with the multiplier of 3 roughly agrees with an observed inflection in the surface temperature response. In this way, the database for the precursory cooling was developed.

Figures 8 and 9 show histograms of the evaluated durations of the precursory cooling, which are based on the multipliers of three and two, respectively. Figures 8 and 9 show that the histogram takes the most probable duration of ~60msec with a relatively large variation of up to ~400msec, and a tendency of a larger variation with a smaller multiplier. The results may indicate qualitatively different behaviors occurring for the duration of 60msec and that of much larger duration.

In order to explain reasons for the relatively large variation observed in the duration distribution, typical behavior of the heat transfer coefficient and surface temperature with a relatively large duration of ~300msec is plotted in **Figures** 10 and 11, respectively. Figures 10 and 11 indicate that the relatively large duration is caused by a temporal change of heat transfer coefficient and temperature between 0.1 and 0.4 sec before rewetting. This temporal change was probably caused randomly by impinging liquid droplets with large impact velocity and/or large fluid volume.

The evaluated most probable duration of ~60msec corresponds to the required time for the surface to be cooled to the rewetting temperature against the stored heat release when above-mentioned random cooling does not occur. This duration did not clearly show the dependence of a thermal-hydraulic parameter such as the rewetting velocity. The evaluated length of the precursory cooling, therefore, showed a linear relation against the rewet velocity as shown in **Figure** 12, where the length is defined as the product of the rewetting velocity and duration which is evaluated using the multiplier of 3. Relatively large lengths shown in Figure 12 correspond to the large variation of the duration described

above. Observed discrete slopes in Figure 12 correspond to the data sampling interval of 10msec.

4.2. Rewetting Front Propagation Velocity

Figure 13 shows the cladding surface temperatures at the t3 timings at each measured location for the rewetting experiments at 7MPa. The temperature before the precursory cooling was generally higher for the lower position because of the difference in the linear axial power density. Those data are plotted against the rewetting velocity in **Figure** 14. The mass flux conditions are expressed using different symbols in Figure 14, which indicates a weak tendency that the rewetting velocity increases with the mass flux. Figure 14 also appears to indicate the existence of the maximum rewetting velocity for a given cladding surface temperature, which envelops the scattered data in Figure 14. The maximum rewetting velocity curve in Figure 14 shows an increase tendency with decrease in the cladding temperature.

Since the typical two-phase flow pattern in the BWR core during the AOOs is an annular-mist flow, the rewetting front propagation is determined by the liquid film propagation. The tendency in Figure 14 may suggest that there also exists the limitation of the rewetting velocity by the maximum heat transfer for sufficiently high cladding temperature. That is, the rewetting occurs when the liquid film arrives at the location when the cladding temperature is not high enough, while the rewetting velocity is limited when the cladding temperature is high enough. This behavior can be understandable by considering steady-state behavior in a system fixed on the rewetting front. For this steady-state condition, the release rate of stored heat should be balanced with the heat transfer rate. In general, the release rate of the stored heat is roughly proportional to the product of the rewetting velocity and superheat of the heater rod, while the maximum heat transfer rate is determined by the maximum wetting temperature and the heat transfer rates

in the wetted and the precursory cooling region. Therefore, the maximum heat transfer rate limits the stored heat release rate and thus the rewetting velocity. This presumption will be investigated in the numerical analysis in the next section.

4.3. Comparison of Rewetting Front Propagation Velocity Data and Analysis

Two dimensional heat conduction analysis results described in the section 3.1 is compared with the experimental data. **Figure** 15 shows the calculated rewetting velocities vs. cladding surface temperatures, compared with the experimental data and changing the length of the precursory cooling region as a calculation parameter. Figure 15 clearly confirms the previously obtained conclusions related to the precursory cooling that dominates the rewetting front propagation. That is, when the precursory cooling is not modeled, the analysis results cannot explain the measured rewetting behavior.

Although the base case results seem to roughly agree with the averages of the wide-scattered data as shown in Figure 15, this comparison is not physically appropriate because the rewetting behavior is presumably determined by the liquid film flow in the annular-mist flow mode that is not taken into account in the present model. Therefore, the agreement between the experimental data and analysis results were not improved even when each data was compared with the analysis result using the measured mass flux and quality instead of a typical value indicated by the base case condition in Table 2. On the other hand, the maximum heat transfer near the rewetting front may be determined more locally. Therefore, the present model may be more appropriate for the comparison with the maximum rewetting velocity. **Figures** 16 and 17 show calculated rewetting velocities vs. cladding surface temperatures changing the rewetting temperatures and heat fluxes as a calculation parameter, respectively. Figures 16 and 17 clearly indicate significant effects of the heat transfer near the wetting front. It should be noted that the maximum propagation velocity agreed well by the present sensitivity calculation with a parameter giving the largest heat

transfer rate near the rewetting front, which indicates a possibility that the maximum propagation velocity may be expressed by appropriate heat transfer correlations expressed by the local parameters.

5. Discussion

5.1. Transition Boiling Heat Transfer Correlation

One of possible causes for the underprediction of the rewetting velocity for the case without the model for the precursory cooling was the use of the Groeneveld correlation, which was developed using the data obtained at relatively high wall superheat. That is, if the increase of heat transfer had been predicted appropriately corresponding to the decrease in the surface temperature due to the axial conduction, the rewetting velocity would have been predicted better. The strong dependency of the surface temperature on the heat transfer is a fundamental nature of the transition boiling mode. In order to investigate this possibility, sensitivity calculations were conducted using a heat transfer correlation developed in our previous study from the steady-state post-BT experimental data including those under low superheat conditions [3].

The result showed no differences by the use of the above correlation, probably because the region affected by the axial heat conduction was so small that the difference of the heat transfer correlations did not effectively change the heat transfer immediately before rewetting. This indicates the precursory cooling model should take into account the enhancement of the heat transfer as a function of the distance from the front.

5.2. Uncertainty of Evaluated Precursory Cooling Duration

The durations of precursory cooling had the most provable value of ~60msec. The uncertainty of the evaluated duration for such a rapid transient was analyzed based on the procedure using the 3-D and 1-D analyses described previously. This uncertainty affects the

extent of the precursory cooling region and the evaluation for the initial surface temperature before the precursory cooling. For the 3-D calculation, the rewetting velocity of 20cm/s and the precursory cooling length of 1cm were assumed, which was equivalent to the duration of 50msec. The other condition was the same as the base case described in the previous section.

Figure 18 shows temperatures at the surface and the simulated T/C location evaluated by the 3-D analysis, which are compared with those evaluated by the 1-D analysis. The onset of the precursory cooling started at 0.2 sec for the 3-D analysis, after which relatively large differences in surface temperatures were observed between the two analyses. Similarly, the heat flux based on the 1-D analysis is compared with that obtained in the 3-D analysis in **Figure** 19. The timing of taking a peak was delayed for the 1-D analysis by 24msec, while the onset time for the precursory cooling was also delayed by 30msec. Here, the onset time is represented by the t3 timing defined in the previous section. As a result, the duration of precursory cooling evaluated by the 1-D analysis was 12% larger than that specified in the 3-D calculation for this condition.

Additionally, one case was calculated for the precursory cooling duration of 100 msec. **Table** 3 summarizes those results of the differences of the precursory cooling duration for the two cases. Because of the volume of the temperature sense region of the thermocouple and its location from the surface, it is inevitable that the evaluated timings of the peak heat flux and the precursory cooling onset are calculated later in the 1-D analysis based on the simulated T/C data. Quantitative differences, however, did not exceed by 50% for those cases. Those results indicate that the magnitude of the duration may be roughly evaluated using the present procedure.

5.3. Technical Issues Identified

First of all, it should be noted that the mechanism of the precursory cooling is not known. A possible mechanism is a formation of the liquid rivulet after the liquid film

thickness becomes below a critical value to spread uniformly on the surface. Oscillatory formations of the rivulets near the rewet front may explain the characteristics of the precursory cooling with high heat transfer coefficient existing only in the vicinity of the rewetting front. The impingement of liquid droplets on the near-surface-region may not explain the characteristics of the precursory cooling, since it seems to occur randomly.

The present study has indicated that the rewetting propagation velocity is limited by the maximum heat transfer in the vicinity of the rewetting front. The maximum heat transfer is determined by the heat transfer for the wetted region, the maximum liquid superheat at the rewetting front and the precursory cooling. Those heat transfer behaviors were not sufficiently studied for the present condition characterized by transient, high-pressure and high-flow rate: the heat transfer correlation for the wetted region such as the Chen correlation is generally developed using the steady-state data; the maximum superheat has been investigated primarily at low pressure and stagnant conditions. The significance of the precursory cooling near the rewetting front was identified in our previous study and was not studied extensively at high pressure and high heat flux. The study for those heat transfer behaviors is, therefore, required to develop a prediction model for the maximum rewetting front velocity. It is also interesting to investigate whether the maximum heat transfer is simply modeled using locally available parameters, which is an important characteristic for the use in the two-field model codes such as RELAP5.

The prediction of the liquid film propagation is required for the prediction of the rewetting velocity when the cladding surface temperature is not high enough. This behavior is affected by time-dependent liquid film behavior in the region upstream of the rewetting front and cannot be described in the models based on the local parameters. The behavior is generally evaluated using the two-fluid three-field model in which the liquid film flow is evaluated from the mass balance affected by the liquid entrainment, droplets deposition and phase change. Several codes based on the two-fluid three-field model have been developed

and used for the detailed evaluation, which are not validated sufficiently to be used in the safety review.

Core heat transfer is known to be significantly affected by the spacer especially for the high-heat flux condition. The heat transfer performance that is typically expressed as the critical heat flux is generally confirmed by large-scale heat transfer experiments using the actual geometry. On the other hand, the heat transfer models used for the accidental analysis basically do not take into account the spacer effect. The negligence of the spacer effect may be justified for the low vapor velocity long after the core scram. Since the thermal-hydraulic condition beyond AOO is characterized by the high core power, the effect of the spacer is required to be better clarified for a safety review: at least the conditions where the spacer effect can be neglected should be clarified.

The rewetting velocity is determined by a balance of the stored heat release rate and the cooling rate. The stored heat release is dependent on the physical properties, and thus, the effect of the difference between the heater rod and nuclear fuel should be clarified to better understand the applicability of the experiments to the actual reactor conditions. It should be noted that this is not discussed in the AESJ standard in which two rewetting propagation models are recommended.

6. Conclusions

Our previous study investigated the rewetting behavior of dryout fuel surfaces during transients beyond anticipated operational occurrences (AOOs) for BWRs, which indicated the rewetting velocity was significantly affected by the precursory cooling defined as cooling immediately before rewetting. The present study further investigated the previous experiments by conducting additional experimental and numerical analyses to characterize the precursory cooling. From the study, we obtained the following conclusions:

1. The duration of the precursory cooling was defined from the two timings of the onset of the precursory cooling and the maximum heat flux. The latter was determined directory from the one-dimensional heat conduction analysis using the measured surface temperature as a boundary condition. The former was determined as a time when the evaluated heat transfer coefficient exceeded a product of a constant multiplier and the average heat transfer coefficient away from the rewetting front. By using an appropriate multiplier, a database for the precursory cooling was established.
2. A distribution of the evaluated durations of the precursory cooling took the most probable value at ~60msec and varied up to 400msec. The data showing the relatively large value of the duration appears to be randomly affected by liquid droplets. The duration of ~60msec corresponded to the precursory cooling length of up to ~15mm.
3. The rewetting velocity was investigated as a function of the cladding temperature at the onset timing for the precursory cooling. The results have indicated that the measured propagation velocity has the maximum for a given temperature, which appears to be limited by the maximum heat transfer rate near the rewetting front.
4. This limitation was consistently reproduced in the numerical analysis using heat transfer models for the precursory cooling, the maximum wetting temperature, and the heat transfer coefficients in the wetted region.
5. The uncertainty in evaluating the precursory cooling was analyzed in the three-dimensional heat conduction analysis taking into account the location, physical property and size of the temperature sense region in the sheath-type thermocouple. The results have indicated that the duration of the precursory cooling can be roughly evaluated by the present analysis method.
6. The following technical issues were identified as discussed in Section 5.3, which requires further investigation to improve phenomenological understanding and develop the rewetting front propagation model:

- Physical mechanism of the precursory cooling
- Models to predict the heat transfer behavior in the vicinity of the rewetting front, including the maximum wetted temperature, the heat transfer coefficients for the wetted region and the precursory cooling
- Models development and establishment of database for validation for the two-fluid three-field models to predict transient film flow of the annular-mist flow
- Effects of the spacer and rod physical property to improve the understanding on the scaling effects

Nomenclature

AESJ	Atomic Energy Society of Japan
AOO	Anticipated operational occurrence
CHF	Critical heat flux
JAEA	Japan Atomic Energy Agency
Post-BT	Post boiling transition
t1,t2,t3 timings	Timings at which the heat transfer coefficient exceeds the average between 1 and 2 sec before rewetting multiplied by 1.3, 2 and 3, respectively
T/C	Thermocouple

References

[1] Atomic Energy Society of Japan. 2003 Standard for assessment of fuel integrity under anticipated operational occurrence in BWR power plants: 2003. Tech. Rep. AESJ-SC-P002:2003, Subcommittee on the core and fuel, the power reactor technical

committee and the standards committee. (in Japanese). 2003.

[2] Sibamoto Y, Maruyama Y, Nakamura H. Measurement and analysis for rewetting velocity under Post-BT conditions during anticipated operational occurrence of BWR. J. Eng. Gas Turbines Power, 2010; 132: 102909–1–8.

[3] Sibamoto Y, Maruyama Y, Yonomoto T, Nakamura H. Core heat transfer coefficients immediately downstream of the rewetting front during anticipated operational occurences for BWRs, J. Nucl. Sci. Technol., 2011; 48(3): 440-453 .

[4] Sibamoto Y, Maruyama Y, Yonomoto T. Rewetting front propagation under anticipated operational occurrences for boiling water reactors –development of two-dimensional analytical model. J. Nucl. Sci. Technol. 2013; 50:148–159.

[5] Thurgood, M. J. et al., S., COBRA/TRAC-A Thermal-hydraulic code for transient analysis of nuclear reactor vessels and primary coolant systems, 1983, NUREG/CR-3046.

[6] Heimsund BO. matrix-toolkits-java, Available from: https://github.com/fommil/matrix-toolkits-java

[7] Chen J.C. Correlation for boiling heat transfer to saturated fluids in convective flow, I&EC Process Des. Development. 1966; 5:322-329.

[8] Groeneveld D.C. An investigation of heat transfer in the liquid deficient regime, AECL 3281, 1969.

[9] Lienhard JH. Correlation for the limiting liquid superheat, Chem. Eng. Sci., 1976; 31: 847–849.

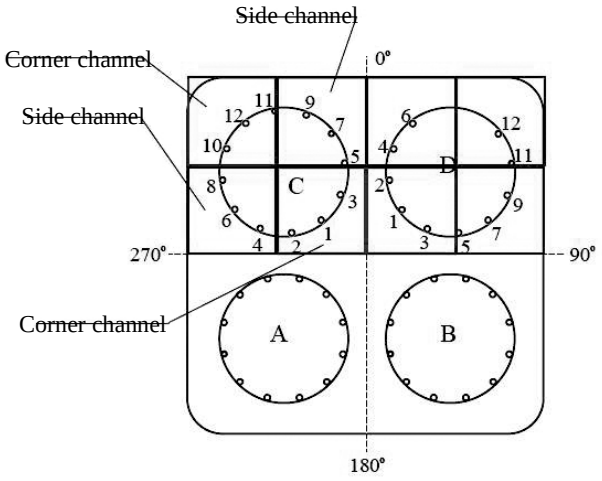

Figure 1. Crosssectional view of the 2x2 bundle test section.

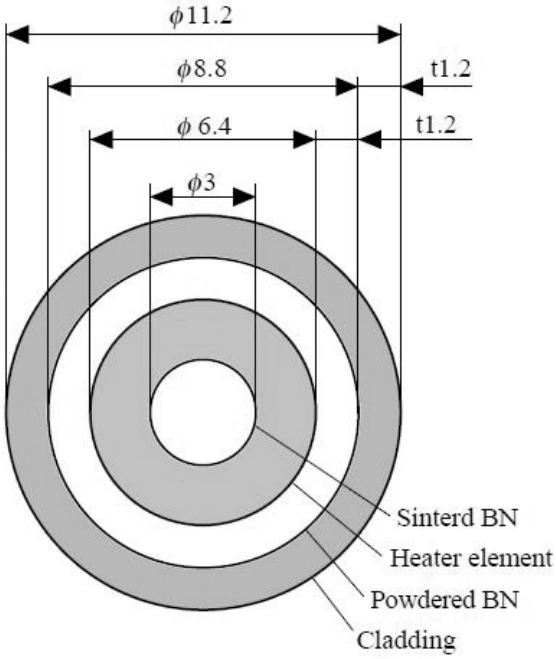

Figure 2. Crosssectional view of the heater rod.

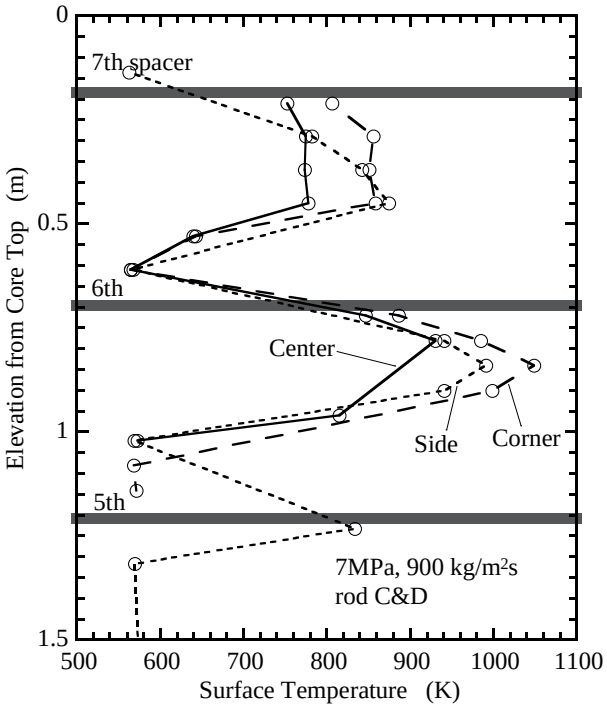

Figure 3. Typical steady-state cladding surface temperature profiles under the post-BT condition.

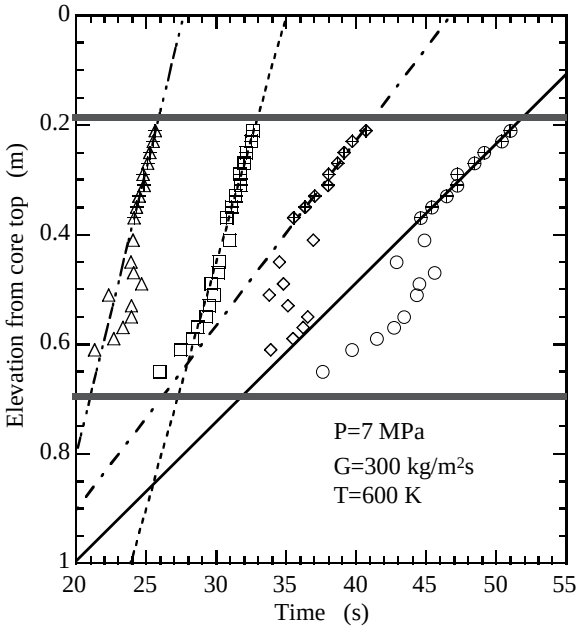

Figure 4. Typical rewetting front propagation behavior

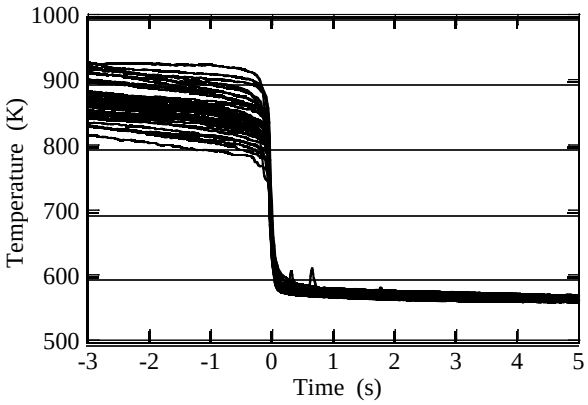

Figure 5. Cladding temperatures at 0.821 m from the core top measured for all rewetting experiments at 7 MPa: The time zero corresponds to the timing at which evaluated heat flux took a maximum.

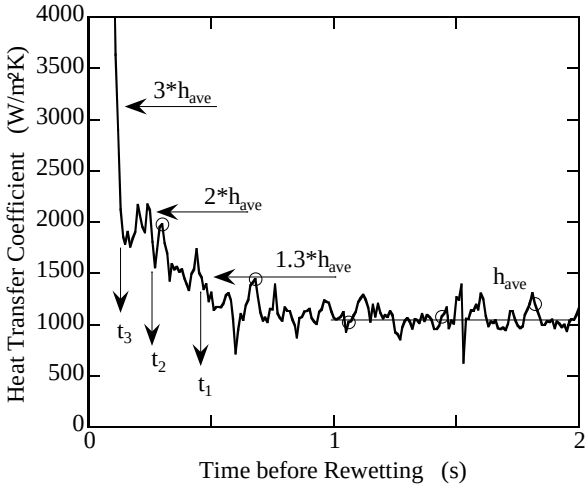

Figure 6. Typical response of heat transfer coefficient before rewetting. : Timings of t1, t2 and t3 are defined as timings at which the heat transfer coefficient exceeds the average between 1 and 2 sec before rewetting multiplied by 1.3, 2 and 3, respectively.

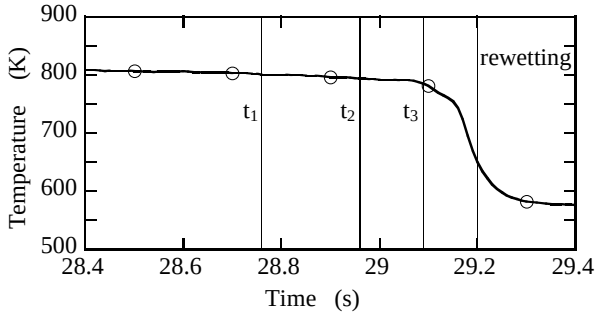

Figure 7. Typical cladding surface temperature compared with timings of t1, t2 and t3.

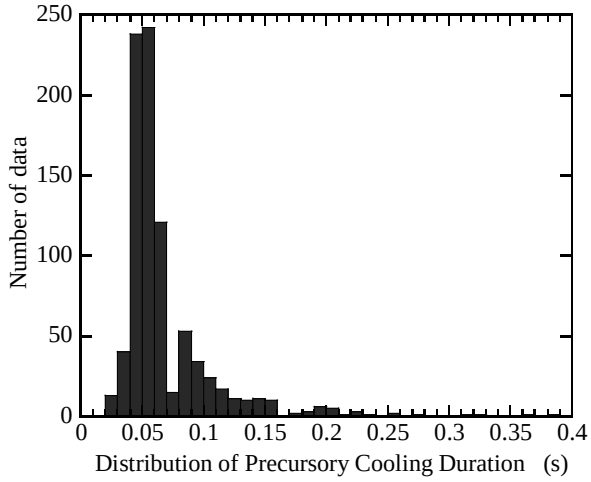

Figure 8. Distribution of precursory cooling duration based on t3 timing.

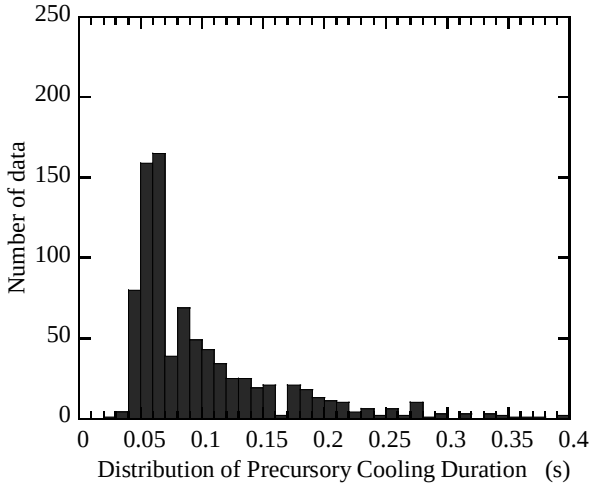

Figure 9. Distribution of precursory cooling duration based on t2 timing.

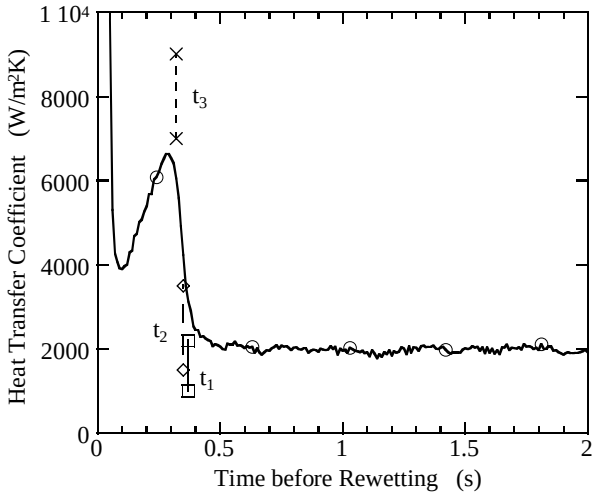

Figure 10. Typical response of heat transfer coefficient with relatively large duration of precursory cooling.

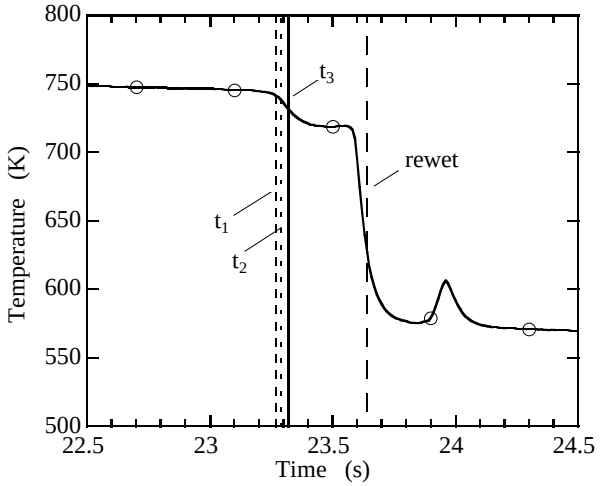

Figure 11. Typical response of cladding surface temperature with relatively large duration of precursory

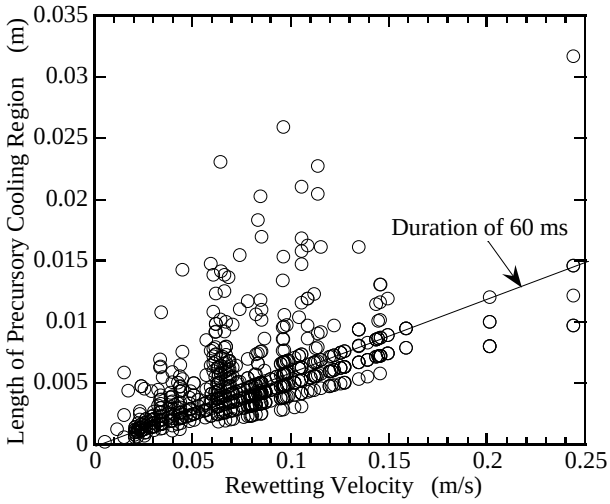

Figure 12. Evaluated lengths of precursory cooling based on t3 timing vs. rewetting velocities

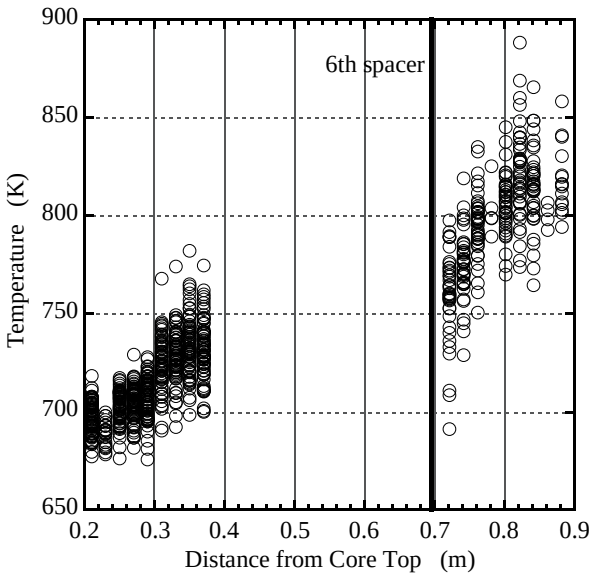

Figure 13. Cladding temperatures at the t3 timing vs. distances from the core top.

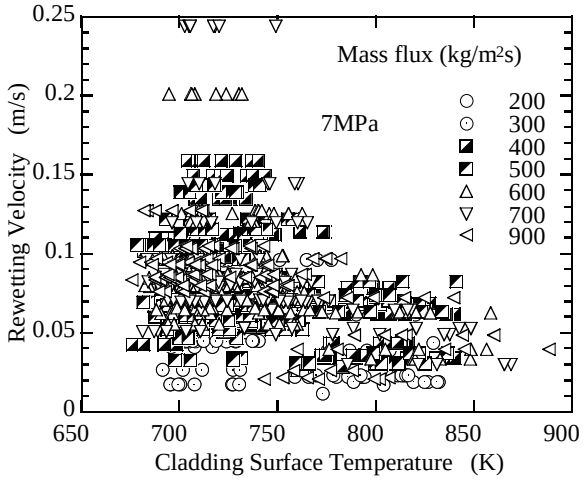

Figure 14. Rewetting velocities vs. cladding surface temperatures

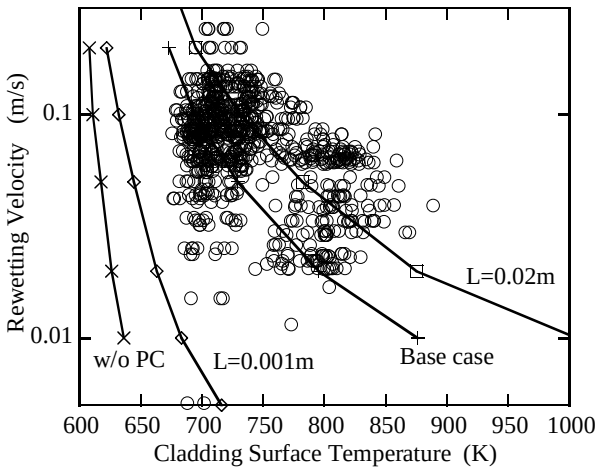

Figure 15. Comparison of analyzed and measured rewetting velocities vs. cladding temperatures: effects of the length of precursory cooling

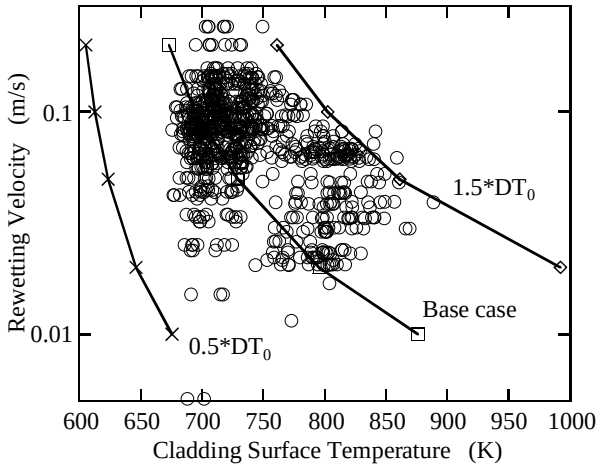

Figure 16. Comparison of analyzed and measured rewetting velocities vs. cladding temperatures showing effects of rewetting superheat temperature (DT0).

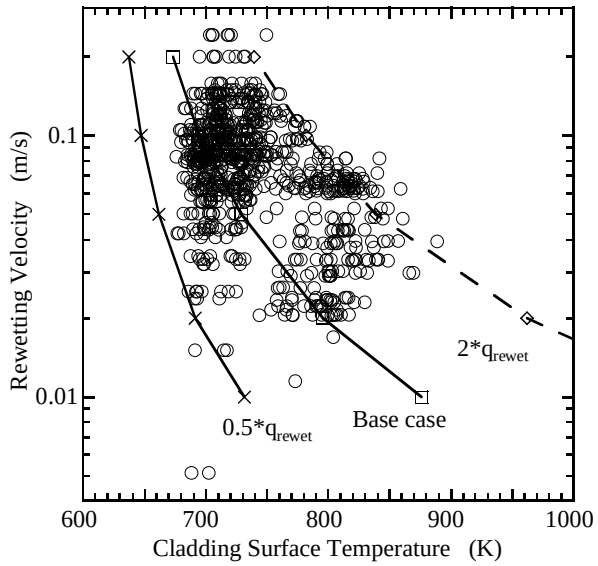

Figure 17. Comparison of analyzed and measured rewetting velocities vs. cladding temperatures showing effects of rewet heat flux (qrewet).

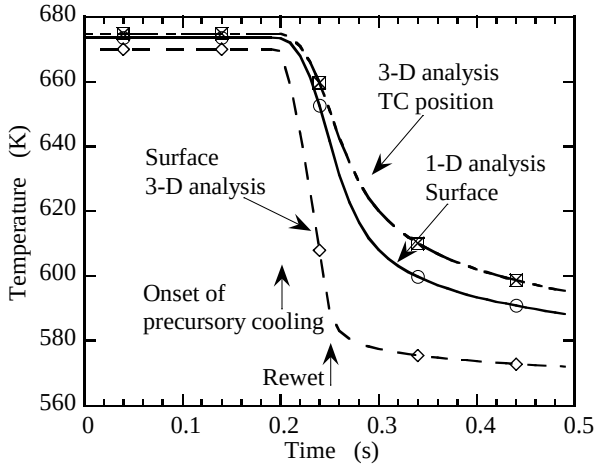

Figure 18. Comparison of cladding temperatures analyzed by the 3-D and 1-D models: The 1-D analysis was based on the temperature at the T/C location calculated by the 3-D model.

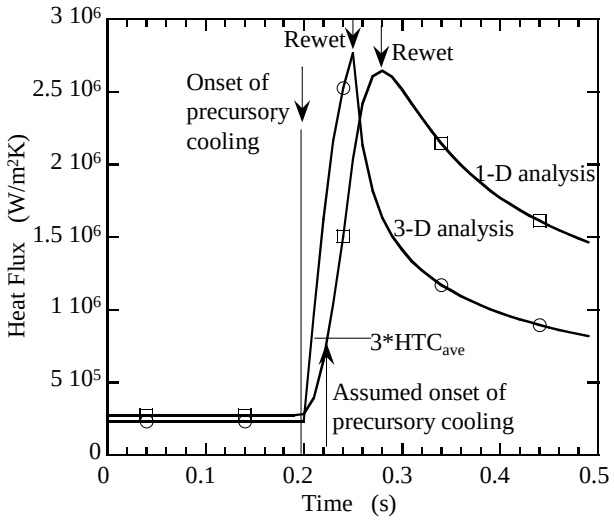

Figure 19. Comparison of surface heat fluxes analyzed by the 3-D and 1-D models for the error evaluation of the precursory cooling duration.

Table 1. Experimental conditions.

Parameters	Conditions
Pressure	7 MPa
Mass flux	200 to 900 kg/m^{2}s
Cladding temperature	< 1073 K

Table 2. Base case calculation conditions.

Parameters	Conditions
Pressure	7 MPa
Mass flux	500 kg/m^{2}s
Quality	0.7
Rewetting superheat temperature	46 K

Table 3 Errors of evaluated durations of the precursory cooling

3-D analysis	1-D analysis based on simulated T/C data		
Specified duration	Error		
	Onset time	Peak HF time	Duration
50 ms	24 ms	30 ms	6 ms (12%*)
100 ms	37 ms	5 ms	-32 ms (-32%*)

HF: heat flux, *: relative value